Journal of Materials Science and Chemical Engineering, 2015, 3, 17-25
Published Online April 2015 in SciRes. http://www.scirp.org/journal/msce
http://dx.doi.org/10.4236/msce.2015.34003

Preparation and Photocatalytic Properties of $LnBaCo_2O_{5+\delta}$ (Ln = Eu, Gd, and Sm)

Bingqian Han[1], Yuxiu Li[1], Nan Chen[1], Dongyang Deng[1], Xinxin Xing[1], Yude Wang[1,2*]

[1]Department of Materials Science and Engineering, Yunnan University, Kunming, China
[2]Yunnan Province Key Lab of Micro-Nano Materials and Technology, Yunnan University, Kunming, China
Email: *ydwang@ynu.edu.cn

Received 26 February 2015; accepted 17 April 2015; published 21 April 2015

Abstract

A new type of photocatalytic material, double-perovskite oxides, $LnBaCo_2O_{5+\delta}$ (Ln = Eu, Gd, and Sm) was synthesized via a conventional solid-state reaction process using Ln_2O_3, $BaCO_3$ and Co_2O_3 as raw materials. X-ray diffraction results show that the crystalline structures are a pure orthorhombic lattice and are consistent with $LnBaCo_2O_{5+\delta}$ microparticles. The photocatalytic activity of the $LnBaCo_2O_{5+\delta}$ (Ln = Eu, Gd, and Sm) powders was further demonstrated in the degradation of Congo red (CR) under ultraviolet light irradiation with the dye solution concentration of 25 or 50 $mg \cdot L^{-1}$. The double-perovskite oxides $LnBaCo_2O_{5+\delta}$ show a certain photocatalytic activity during the degradation of CR under ultraviolet light, which means that they are one kind of the promising photocatalytic materials for the degradation of the azo dyes.

Keywords

Double-Perovskite, $LnBaCo_2O_{5+\delta}$, Photocatalysis, Congo Red

1. Introduction

With the society and economic development, the problem of environmental pollution is outstanding day by day. Especially, the contamination of water due to color effluents coming from different industries, such as textiles, dyestuff, and paper, which are toxic and low-biodegradable, discharges into the aquatic systems and leads to the serious destroy of the survival environment as well as serious damage to human health [1]-[5]. Among these pollution, azo dyes, characterized by the presence of the N=N linkage, are the mostly and frequently used for colorization in textile industries [6]. Faced with the global environmental pollution, the process as efficient as possible in the azo dyes degradation has widely been pursued [7]. Several studies of physical, chemical and bio-

*Corresponding author.

How to cite this paper: Han, B.Q., Li, Y.X., Chen, N., Deng, D.Y., Xing, X.X. and Wang, Y.D. (2015) Preparation and Photocatalytic Properties of $LnBaCo_2O_{5+\delta}$ (Ln = Eu, Gd, and Sm). *Journal of Materials Science and Chemical Engineering*, **3**, 17-25.
http://dx.doi.org/10.4236/msce.2015.34003

logical methods have been carried out. However, since their very stable and complex aromatic structures, the traditional treatment means used for azo dyes effluents are sometimes ineffective, non-destructive and merely transfer pollutants from water to another phase, resulting in secondary pollution, and even generating greater toxicity aromatic amine materials [8]-[10]. In recent years, the photocatalytic process on semiconducting materials has greatly been concerned because it provides a green way to directly degrade waste water pollutants [11]. As a result, numerous semiconductor photocatalytic materials, such as TiO_2 [12], SnO_2 [13], ZnO [14], and $BiVO_4$ [15], have been developed and applied in photocatalytic degradation of organic pollutants due to their high efficiency, commercial availability and high chemical stability.

Perovskite oxides with the general formula of ABO_3 in which A-site (with ionic radius of larger than 1.0 Å) is a rare-earth or an alkali-earth element and B-site (having ionic radius in the order of 0.6 - 0.8 Å) is typically a 3D transition metal become the hotspot of material science because of their stable structure and unique physical and chemical properties [16]. The ideal perovskite ABO_3 has a cubic crystal structure, which is composed of a three-dimensional framework of eight corner-sharing BO_6 octahedrons. Among the structure, BO_6 octahedron is often considered as the basic cell and B-site cation locates in octahedral vacancy while A-site cation fills the twelve coordinate cavities formed by BO_6 network [17] [18]. Due to their unique properties, such as various types of oxygen vacancy order, intrinsic oxygen reduction reaction activity, high conductivity and magnetic properties, perovskites have been used in solid oxide fuel cells, oxygen separation, membrane reactor for partial oxidation of methane to syngas and also used as catalysts for controlled partial hydrocarbon oxidation and photocatalysis [19]-[21]. Especially, their high performances in photocatalytic reactions, such as overall water splitting and photo degradation of organic pollutants, attracted much attention because of their narrower band gap (often less than 3.0 eV) which could be easily excited under visible light or ultraviolet light irradiation [22]. As a photocatalyst, perovskites, such as $SrSnO_3$ [23], $SrTiO_3$ [24] and $LaTiO_3$ [25], have been extensively studied in the field of photo degradation of organic pollutants.

Double-perovskite oxides which named after perovskites ABO_3 are a large family and have wide application fields. Among them, the oxygen deficient ordered double perovskite cobaltates with the general formula $LnBaCo_2O_{5+\delta}$ have drawn significant interest as potential IT-SOFC (Intermediate Temperature-Solid Oxide Full Cell) cathodes, chemical gas censors, magnetic and oxygen permeation materials because of their high electronic conductivity, oxygen transport properties, oxygen surface exchange coefficient and superior oxide ionic diffusivity [26]-[29]. The crystal structures of these oxides are formed by stacking sequence $CoO_2|LnO_\delta|CoO_2|BaO|CoO_2$ along the c direction, and the oxygen vacancies are mainly localized into LnO_δ layer. Transformation of a simple cubic perovskite with randomly occupied A-sites into a layered crystal with alternating lanthanide and alkali-earth planes reduces the strength of oxygen binding and provides disorder-free channels for ionic motion [30]. Since perovskite oxides possess high photocatalytic performances, as with close links to the perovskite compounds, double-perovskite oxides can be conjectured that they are a kind of potential photocatalytic material. Nevertheless, little work has been carried out to investigate their photocatalytic performances.

In this paper, the mainly research is focused on the preparation process and removal properties of organic pollutants CR from the wastewater using the double-perovskite oxides $LnBaCo_2O_{5+\delta}$ (Ln = Eu, Gd, and Sm).

2. Experimental

2.1. Materials Synthesis

All the chemical reagents used in the experiments were obtained from commercial sources as guaranteed-grade reagents and used without further purification and treatment.

$LnBaCo_2O_{5+\delta}$ (Ln = Eu, Gd, and Sm) powders were prepared by a conventional solid-state reaction method. Ln_2O_3, $BaCO_3$ and Co_2O_3 served as the starting materials for the necessary metal ions. The process flow chart is shown in **Figure 1**. Typically, Ln_2O_3, $BaCO_3$ and Co_2O_3 powders were mixed in stoichiometric ratios and thoroughly ground in an agate mortar using ethanol as a solvent for 1 h. After the evaporation of ethanol, the mixed powders were calcined at 1000˚C for 6 h under the air atmosphere and then slowly cooled down to room temperature in the furnace.

2.2. Materials Characterization

The crystal structures of the synthesized materials were characterized by X-ray powder diffraction (XRD) using

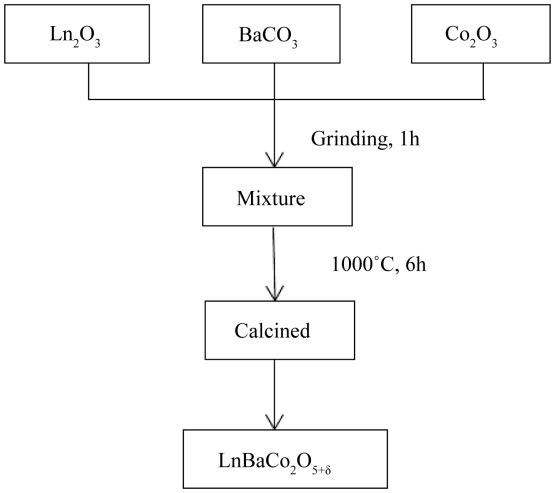

Figure 1. Technological synthesis process of $LnBaCo_2O_{5+\delta}$ (Ln = Eu, Gd, and Sm) powders via solid-state reaction method.

a Rigaku D/Max-3B instrument with copper target and Kα radiation (λ = 1.54056 Å). The accelerating voltage and applied current were 40 kV and 200 mA. The samples were scanned from 10˚ to 90˚ (2θ) in steps of 0.02˚.

2.3. Measurement of Photocatalytic Activity

CR ($C_{32}H_{22}N_6Na_2O_6S_2$, molecular weight: 696.67 g·mol^{-1}, from Guangzhou Reagent Corporation, China) was used as a model dye to evaluate the photocatalytic activity of the $LnBaCo_2O_{5+\delta}$ (Ln = Eu, Gd, and Sm) samples. The degradation tests of CR were conducted in an aqueous solution at room temperature under ultraviolet light irradiation with the dye solution concentration of 25 or 50 mg·L^{-1}. In a typical degradation process, under ultraviolet light irradiation and stirring conditions, 20 mg of the synthesized samples were added into 50 mL CR aqueous solutions with an initial concentration of 25 or 50 mg·L^{-1} in a quartz beaker, respectively. At a given time, 4 mL of the dispersion was continually extracted and subsequently centrifuged to separate $LnBaCo_2O_{5+\delta}$ powders and dye solutions at 4000 rev·min^{-1} for 30 min. The reaction mixtures were irradiated by a Xe-lamp (30 W) with the wavelength range of 320 - 400 nm in which a peak wavelength of 365 nm for UV light and 400 - 800 nm for visible light, and magnetically stirred throughout the photocatalytic experiment under air. The initial concentration (C_0) and the instant concentration (C) of the aqueous solution of CR were determined with a UV-2401PC spectrophotometer at λ_{max} = 498 nm. The degradation rate of CR dye was calculated as C/C_0.

3. Results and Discussion

3.1. The Crystal Structures of the As-Synthesized Samples

Figure 2 shows the X-ray diffraction patterns of the oxides which prepared from the appropriate chemical precursors via calcination at 1000˚C for 6 h under an air atmosphere. The XRD patterns of samples with the nominal compositions of $LnBaCo_2O_{5+\delta}$ (Ln = Eu, Gd, and Sm) are represented at a single-phase double-perovskite without any impurity phase. All the diffraction peaks of LnBCO samples can be indexed well with orthorhombic structure $EuBaCo_2O_{5.52}$ (JCPDS No. 53-0136, a = 3.915 Å, b = 3.882 Å, c = 7.549 Å), $GdBaCo_2O_{5.42}$ (JCPDS No. 53-0135, a = 3.918 Å, b = 3.879 Å, c = 7.545 Å), $SmBaCo_2O_{5.54}$ (JCPDS No. 53-0133, a = 3.913 Å, b = 3.889 Å, c = 7.576 Å), space group Pmmm, and these findings are in agreement with previously published reports [31]-[33].

3.2. The Photocatalytic Activity of the LnBCO Powders

The as-synthesized $LnBaCo_2O_{5+\delta}$ (Ln = Eu, Gd, and Sm) powders with well crystal were used for photocatalytic tests under ultraviolet light irradiation. CR was used as a test contaminant since it has been extensively used as

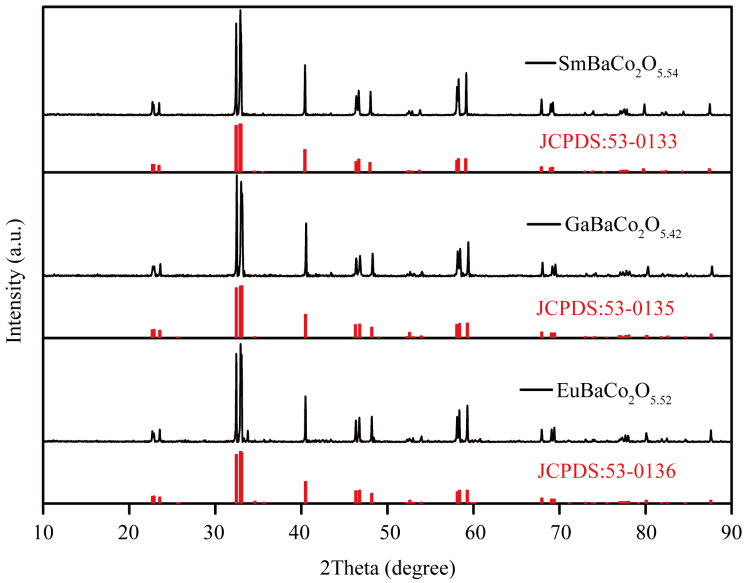

Figure 2. X-ray diffraction analysis of the $LnBaCo_2O_{5+\delta}$ (Ln = Eu, Gd, and Sm) powders.

an indicator for the photocatalytic activity. After photocatalysis experiments, we found that double-perovskite oxides $LnBaCo_2O_{5+\delta}$ could remove the CR effectively, which mean they have photocatalytic properties. **Figure 3** shows the photodegradation rate of CR solutions with different initial concentration in the presence of samples. From **Figure 3(a)**, it is easy to see that the degradation rate of CR solutions (C_0 = 25 mg·L^{-1}) by $EuBaCo_2O_{5.52}$ is rapid at the first 16 h of the reaction time. Following the rapid degradation, the rate decreased and the decolorization efficiency was 92.6% for 24 h. The other two samples, $GdBaCo_2O_{5.42}$ and $SmBaCo_2O_{5.54}$, display similar photocatalytic degradation rates of CR comparing with $EuBaCo_2O_{5.52}$. In general, the catalytic activity is tightly related to the structure of the catalyst [34]. Double-perovskite oxides $LnBaCo_2O_{5+\delta}$ is a kind of distorted perovskite structure which is often caused by the excessive absence of O^{2-} ion. The same structure can explain the phenomenon of similar photocatalytic property of $EuBaCo_2O_{5.52}$, $GdBaCo_2O_{5.42}$ and $SmBaCo_2O_{5.54}$. And likewise, as shown in **Figure 3(b)**, because of the same reason, the three samples have similar photocatalytic degradation rates of a higher concentration of CR solutions (C_0 = 50 mg·L^{-1}) except the time of photodegradation extended to 60 h.

To further clarify the photocatalytic performance and mechanism of CR, the continuous UV-Vis spectra of the centrifuged solution after catalytic reactions at the different intervals were used to record and in contrast to initial CR solution. **Figure 4** displays the UV-Vis absorption spectra of CR solutions (C_0 = 25 or 50 mg·L^{-1}) before and after treatment with as-synthesized $LnBaCo_2O_{5+\delta}$ (Ln = Eu, Gd, and Sm) powders. From the UV-vis absorbance spectrum of CR initial solution, we can see three absorbance peaks at 241, 342 and 498 nm, respectively. The peaks at 241 nm and 342 nm are attributed to benzene ring and naphthalene ring structures, while the peak at 498 nm is attributed to the azo bonds of CR molecule [35]. The characteristic absorption peaks of CR at 342 nm and 498 nm were chosen as the parameter that was monitored. As shown in **Figure 4**, in the presence of $LnBaCo_2O_{5+\delta}$ (Ln = Eu, Gd, and Sm) powders, all absorption peaks went down dramatically along with increasing degradation time and correspondingly the solution became decolorized from red to near colorless. The amplitude of the characteristic peaks continuously decreased with respect to the reaction time and finally to disappear in **Figure 4** suggests that the azo bonds and the naphthyl rings were destroyed to form phenyl derivatives. UV light illumination of the aqueous CR solution in the presence of $LnBaCo_2O_{5+\delta}$ (Ln = Eu, Gd, and Sm) powders causes the absorption bands of the CR dye in the visible region to disappear basically, which indicates that the dye is degraded completely. When $LnBaCo_2O_{5+\delta}$ (Ln = Eu, Gd, and Sm) powders used to degrade CR aqueous solutions, the color of solution was bleached and the absorption of solution at 498 nm was close to zero. In accordance with changes of the absorbance intensity at 498 nm, the decolorization efficiency of 25 mg·L^{-1} CR solution in the presence of $LnBaCo_2O_{5+\delta}$ (Ln = Eu, Gd, and Sm) powders after 3 h degradation reaction was

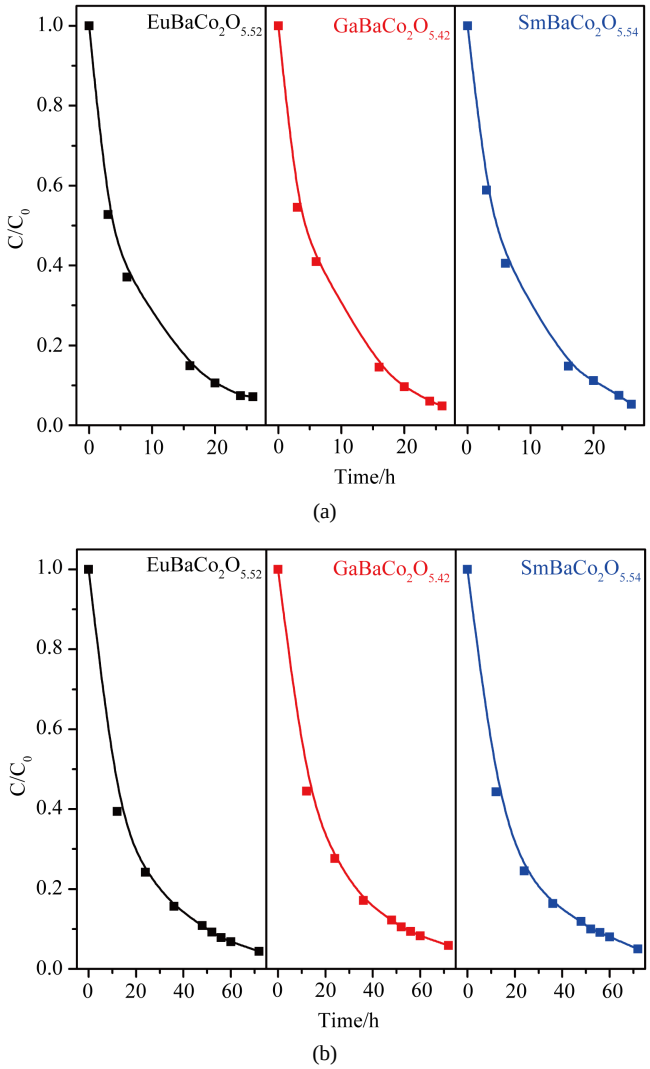

Figure 3. The degradation rate of CR solutions with different initial concentration ((a) 25 mg·L^{-1} and (b) 50 mg·L^{-1}) under ultraviolet light irradiation at room temperature in the presence of $EuBaCo_2O_{5.52}$, $GdBaCo_2O_{5.42}$ and $SmBaCo_2O_{5.54}$, respectively.

achieved about 47%. Complete decolorization of CR solution (C_0 = 25 mg·L^{-1}) was achieved within 26 h. These results are in agreement with the analysis shown in inset. It is clearly seen that the cardinal red color of starting solution gradually disappears along with increasing the degradation time, which also depicts the degradation process of CR.

The possible catalytic mechanism of $LnBaCo_2O_{5+\delta}$ (Ln = Eu, Gd, and Sm) powders is proposed like that of the perovskite oxides. We suppose the photocatalytic property of double-perovskite is derived from the BO_6 octahedron. In $LnBaCo_2O_{5+\delta}$, 2p-orbit of O^{2-} constitutes the valence band, while the 3d-orbit of Co^{3+} constitutes the conduction band. Under the ultraviolet light irradiation, the valence bands electrons of $LnBaCo_2O_{5+\delta}$ were excited and transferred into conduction bands, generating highly reactivity electron-hole pairs which can induce oxidation of organic molecule, by leaving holes (h^+) in the valence bands. The hole (h^+) is a strong oxidant on the surface of $LnBaCo_2O_{5+\delta}$ and could oxidize the adsorbed water molecules or hydroxyl ions into ·OH radicals (H_2O or $OH^- + h^+ \rightarrow \cdot OH$) which is highly radicals to oxidize or degrade the adjacent CR dye molecules. At the same time, the adsorbed oxygen reacted with electrons to form $\cdot O_2^-$ superoxide ions ($O_2 + e^- \rightarrow \cdot O_2^-$) which could decompose the organic molecules effectively [23] [36].

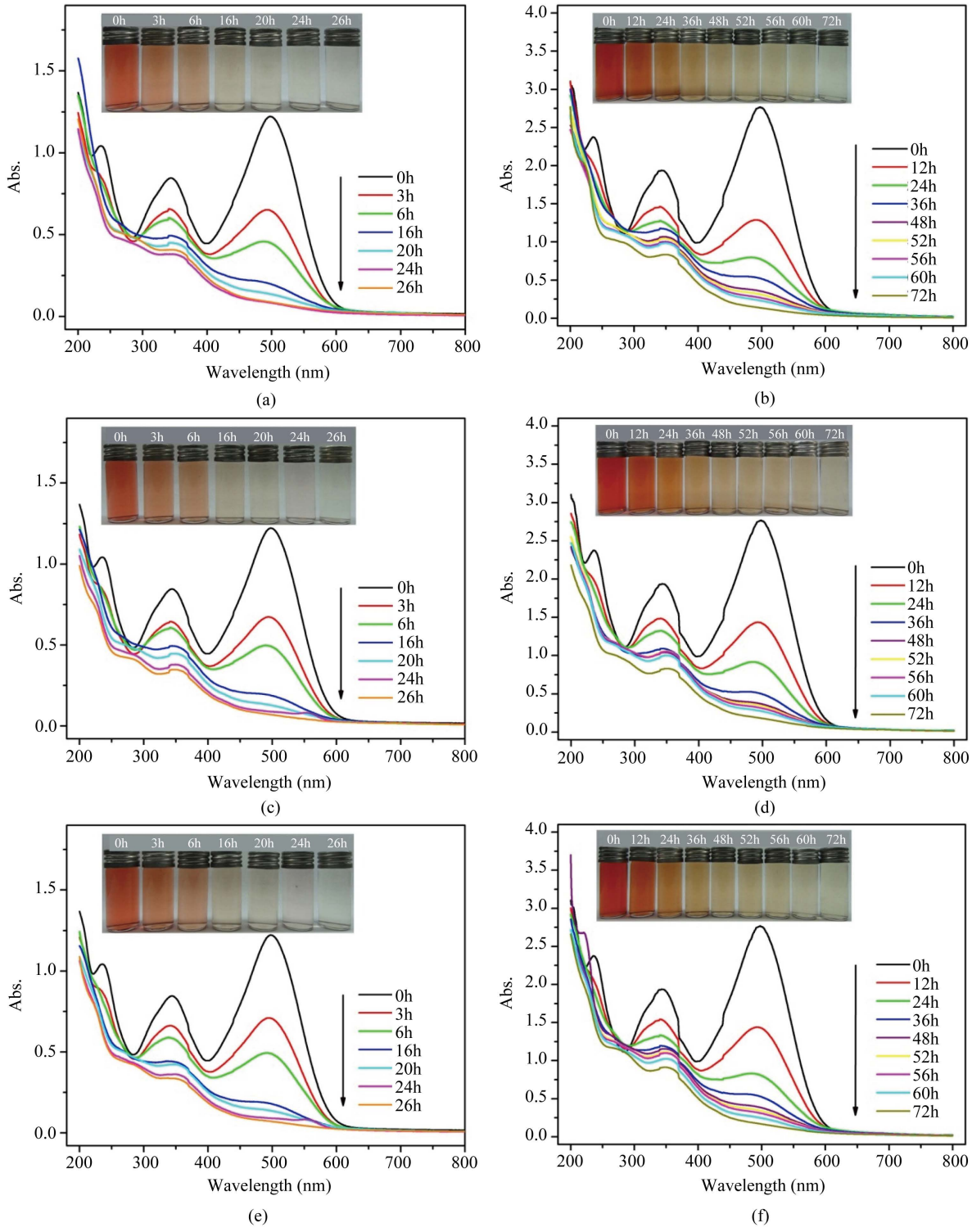

Figure 4. UV-Vis absorption spectra of CR solutions (25 or 50 mg·L^{-1}) before and after treatment with as-synthesized $LnBaCo_2O_{5+\delta}$ (Ln = Eu, Gd, and Sm) powders at different time intervals under ultraviolet light irradiation at room temperature: (a) $EuBaCo_2O_{5.52}$, CR (25 mg·L^{-1}); (b) $EuBaCo_2O_{5.52}$, CR (50 mg·L^{-1}); (c) $GdBaCo_2O_{5.42}$, CR (25 mg·L^{-1}); (d) $GdBaCo_2O_{5.42}$, CR (50 mg·L^{-1}); (e) $SmBaCo_2O_{5.54}$, CR (25 mg L^{-1}); (f) $SmBaCo_2O_{5.54}$, CR (50 mg·L^{-1}). The insets are the photographs of CR solutions (25 or 50 mg·L^{-1}) before and after treatment with as-synthesized $LnBaCo_2O_{5+\delta}$ (Ln = Eu, Gd, and Sm) powders at different time intervals, respectively.

4. Conclusion

Double-perovskite oxides, $LnBaCo_2O_{5+\delta}$ (Ln = Eu, Gd, and Sm) microparticles were successfully prepared by a conventional solid-state reaction method. The samples were characterized by X-ray diffraction (XRD), showing that the resulting particles were highly crystalline LnBCO particles. The photocatalytic activity of the $LnBaCo_2O_{5+\delta}$ (Ln = Eu, Gd, and Sm) powders was investigated by the degradation of CR, and the results revealed that LnBCO had a certain photocatalytic activity, which indicated that they could be a promising photocatalyst for the degradation of organic molecules.

Acknowledgements

This work was supported by National Natural Science Foundation of China (Grant No.51262029), the Key Project of the Department of Education of Yunnan Province (ZD2013006), Program for Excellent Young Talents, Yunnan University (XT412003), Yunnan University Graduate Program for Research and Innovation, and the Department of Science and Technology of Yunnan Province via the Key Project for the Science and Technology (Grant No.2011FA001).

References

[1] Panda, N., Sahoo, H. and Mohapatra, S. (2011) Decolourization of Methyl Orange Using Fenton-like Mesoporous Fe_2O_3-SiO_2 Composite. *Journal of Hazardous Materials*, **185**, 359-365. http://dx.doi.org/10.1016/j.jhazmat.2010.09.042

[2] Zhang, Y.Z., Zheng, J.T., Qu, X.F. and Chen, H.G. (2007) Effect of Granular Activated Carbon on Degradation of Methyl Orange When Applied in Combination with High-Voltage Pulse Discharge. *Journal of Colloid and Interface Science*, **316**, 523-530. http://dx.doi.org/10.1016/j.jcis.2007.08.013

[3] Zhang, F., Liu, Y.J., Cai, Y., Li, H., Cai, X.Y., Djerdj, I. and Wang, Y.D. (2013) A Facial Method to Synthesize $Ni(OH)_2$ Nanosheets for Improving the Adsorption Properties of Congo Red in Aqueous Solution. *Powder Technology*, **235**, 121-125. http://dx.doi.org/10.1016/j.powtec.2012.10.007

[4] Crini, G. (2006) Non-Conventional Low-Cost Adsorbents for Dye Removal: A Review. *Bioresoure Technology*, **97**, 1061-1085. http://dx.doi.org/10.1016/j.biortech.2005.05.001

[5] Ai, L. and Zeng, Y. (2013) Hierarchical Porous NiO Architectures as Highly Recyclable Adsorbents for Effective Removal of Organic Dye from Aqueous Solution. *Chemical Engineering Journal*, **215-216**, 269-278. http://dx.doi.org/10.1016/j.cej.2012.10.059

[6] Saquib, M. and Muneer, M. (2003) Titanium Dioxide Mediated Photocatalyzed Degradation of a Textile Dye Derivative, Acid Orange 8, in Aqueous Suspensions. *Desalination*, **155**, 255-263. http://dx.doi.org/10.1016/S0011-9164(03)00303-5

[7] Hoang, S., Guo, S.W., Hahn, N.T., Bard, A.J. and Mullins, C.B. (2012) Visible Light Driven Photoelectrochemical Water Oxidation on Nitrogen-Modified TiO_2 Nanowires. *Nano Letters*, **12**, 26-32. http://dx.doi.org/10.1021/nl2028188

[8] Mageshwari, K., Nataraj, D., Pal, T., Sathyamoorthy, R. and Park, J. (2015) Improved Photocatalytic Activity of ZnO Coupled CuO Nanocomposites Synthesized by Reflux Condensation Method. *Journal of Alloys and Compounds*, **625**, 362-370. http://dx.doi.org/10.1016/j.jallcom.2014.11.109

[9] Xie, J., Wang, H., Duan, M. and Zhang, L. (2011) Synthesis and Photocatalysis Properties of ZnO Structures with Different Morphologies via Hydrothermal Method. *Applied Surface Science*, **257**, 6358-6363. http://dx.doi.org/10.1016/j.apsusc.2011.01.105

[10] Dong, S., Cui, Y., Wang, Y., Li, Y., Hu, L. and Sun, J. (2014) Designing Three-Dimensional Acicular Sheaf Shaped $BiVO_4$/Reduced Graphene Oxide Composites for Efficient Sunlight-Driven Photocatalytic Degradation of Dye Wastewater. *Chemical Engineering Journal*, **249**, 102-110. http://dx.doi.org/10.1016/j.cej.2014.03.071

[11] Kim, C., Choi, M. and Jang, J. (2010) Nitrogen-Doped SiO_2/TiO_2 Core/Shell Nanoparticles as Highly Efficient Visible Light Photocatalyst. *Catalysis Communications*, **11**, 378-382. http://dx.doi.org/10.1016/j.catcom.2009.11.005

[12] Carp, O., Huisman, C.L. and Reller, A. (2004) Photoinduced Reactivity of Titanium Dioxide. *Progress in Solid State Chemistry*, **32**, 33-177. http://dx.doi.org/10.1016/j.progsolidstchem.2004.08.001

[13] Yin, K., Shao, M.W., Zhang, Z.S. and Lin, Z.Q. (2012) A Single-Source Precursor Route to Ag/SnO_2 Heterogeneous Nanomaterials and Its Photo-Catalysis in Degradation of Congo Red. *Materials Research Bulletin*, **47**, 3704-3708. http://dx.doi.org/10.1016/j.materresbull.2012.06.037

[14] Zhang, J., Deng, S.J., Liu, S.Y., Chen, J.M., Han, B.Q., Wang, Y. and Wang, Y.D. (2014) Preparation and Photocatalytic Activity of Nd Doped ZnO Nanoparticles. *Materials Technology*, **29**, 262-268.

http://dx.doi.org/10.1179/1753555713Y.0000000122

[15] Luo, Y.Y., Tan, G.Q., Dong, G.H., Zhang, L.L., Huang, J., Yang, W., Zhao, C.C. and Ren, H.J. (2015) Structural Transformation of Sm^{3+} Doped $BiVO_4$ with High Photocatalytic Activity under Simulated Sun-Light. *Applied Surface Science*, **324**, 505-511. http://dx.doi.org/10.1021/cr980129f

[16] Peňa, M.A. and Fierro, J.L.G. (2001) Chemical Structures and Performance of Perovskite Oxides. *Chemical Reviews*, **101**, 1981-2017. http://dx.doi.org/10.1016/j.apsusc.2014.10.168

[17] Yang, Y., Sun, Y.B. and Jiang, Y.S. (2006) Structure and Photocatalytic Property of Perovskite and Perovskite-Related Compounds. *Materials Chemistry and Physics*, **96**, 234-239. http://dx.doi.org/10.1016/j.matchemphys.2005.07.007

[18] Wang, Z.L. and Kang, Z.C. (1998) Functional and Smart Materials-Structural Evolution and Structure Analysis. Plenum Press, New York.

[19] Yamamoto, T., Kobayashi, Y., Hayashi, N., Tassel, C., Saito, T., Yamanaka, S., Takano, M., Ohoyama, K., Shimakawa, Y., Yoshimura, K. and Kageyama, H. (2012) $(Sr_{1-x}Ba_x)FeO_2$ ($0.4 \le x \le 1$): A New Oxygen-Deficient Perovskite Structure. *Journal of the American Chemical Society*, **134**, 11444-11454. http://dx.doi.org/10.1021/ja3007403

[20] Suntivich, J., Gasteiger, H.A., Yabuuchi, N., Nakanishi, H., Goodenough, J.B. and Shao-Horn, Y. (2011) Design Principles for Oxygen-Reduction Activity on Perovskite Oxide Catalysts for Fuel Cells and Metal-Air Batteries. *Nature Chemistry*, **3**, 546-550. http://dx.doi.org/10.1038/nchem.1069

[21] Buannic, L., Blanc, F., Middlemiss, D.S. and Grey, C.P. (2012) Probing Cation and Vacancy Ordering in the Dry and Hydrated Yttrium-Substituted $BaSnO_3$ Perovskite by NMR Spectroscopy and First Principles Calculations: Implications for Proton Mobility. *Journal of the American Chemical Society*, **134**, 14483-14498. http://dx.doi.org/10.1021/ja304712v

[22] Yin, J., Zou, Z. and Ye, J. (2003) Photophysical and Photocatalytic Properties of $MIn_{0.5}Nb_{0.5}O_3$ (M = Ca, Sr, and Ba). *The Journal of Physical Chemistry B*, **107**, 61-65. http://dx.doi.org/10.1021/jp026403y

[23] Junploy, P., Thongtem, S. and Thongtem, T. (2013) Photoabsorption and Photocatalysis of $SrSnO_3$ Produced by a Cyclic Microwave Radiation. *Superlattices and Microstructures*, **57**, 1-10. http://dx.doi.org/10.1016/j.spmi.2013.01.008

[24] Ahuja, S. and Kutty, T.R.N. (1996) Nanoparticles of $SrTiO_3$ Prepared by Gel to Crystallite Conversion and Their Photocatalytic Activity in the Mineralization of Phenol. *Journal of Photochemistry and Photobiology A*: *Chemistry*, **97**, 99-107. http://dx.doi.org/10.1016/1010-6030(96)04324-9

[25] Zhang, L.L., Nie, Y.L., Hu, C. and Qu, J.H. (2012) Enhanced Fenton Degradation of Rhodamine B over Nanoscaled Cu-Doped $LaTiO_3$ Perovskite. *Applied Catalysis B*: *Environmental*, **125**, 418-424. http://dx.doi.org/10.1016/j.apcatb.2012.06.015

[26] Kim, J.H. and Manthiram, A. (2008) $LnBaCo_2O_{5+\delta}$ Oxides as Cathodes for Intermediate-Temperature Solid Oxide Fuel Cells. *Journal of the Electrochemical Society*, **155**, B385-B390. http://dx.doi.org/10.1149/1.2839028

[27] Klyndziuk, A., Petrov, G., Kurhan, S., Chizhova, Y., Chabatar, A. and Kunitski, L. (2004) Sensor Properties of Some Perovskite-Like Metal Oxides. *Chemical Sensors*, **20**, 854-855.

[28] Fauth, F., Suard, E., Caignaert, V., Domengès, B., Mirebeau, I. and Keller, L. (2001) Interplay of Structural, Magnetic and Transport Properties in the Layered Co-Based Perovskite $LnBaCo_2O_5$ (Ln = Tb, Dy, Ho). *The European Physical Journal B*: *Condensed Matter and Complex Systems*, **21**, 163-174. http://dx.doi.org/10.1007/PL00011119

[29] Chen, T., Zhao, H.L., Xu, N.S., Li, Y., Lu, X.G., Ding, W.Z. and Li, F.S. (2011) Synthesis and Oxygen Permeation Properties of a $Ce_{0.8}Sm_{0.2}O_{2-\delta}$-$LaBaCo_2O_{5+\delta}$ Dual-Phase Composite Membrane. *Journal of Membrane Science*, **370**, 158-165. http://dx.doi.org/10.1016/j.memsci.2011.01.007

[30] Taskin, A.A., Lavrov, A.N. and Ando, Y. (2005) Achieving Fast Oxygen Diffusion in Perovskites by Cation Ordering. *Applied Physics Letters*, **86**, Article ID: 091910. http://dx.doi.org/10.1063/1.1864244

[31] Zhang, K., Ge, L., Ran, R., Shao, Z.P. and Liu, S.M. (2008) Synthesis, Characterization and Evaluation of Cation-Ordered $LnBaCo_2O_{5+\delta}$ as Materials of Oxygen Permeation Membranes and Cathodes of SOFCs. *Acta Materialia*, **56**, 4876-4889. http://dx.doi.org/10.1016/j.actamat.2008.06.004

[32] Zhang, X.T., Hao, H.S., He, Q.L. and Hu, X. (2007) High-Temperature Electronic Transport Properties of Fe-Doped $YBaCo_2O_{5+\delta}$. *Physica B*: *Condensed Matter*, **394**, 118-121. http://dx.doi.org/10.1016/j.physb.2007.02.027

[33] Yasodha, P., Gayathri, N., Bharathi, A., Premila, M., Sundar, C.S. and Hariharan, Y. (2007) Ce-Substitution Effects in $GdBaCo_2O_{5+\delta}$. *Solid State Communications*, **144**, 215-219. http://dx.doi.org/10.1016/j.ssc.2007.08.033

[34] Wang, Y., Wang, Y., Meng, Y.L., Ding, H.M., Shan, Y.K., Zhao, X. and Tang, X.Z. (2008) A Highly Efficient Visible-Light-Activated Photocatalyst Based on Bismuth- and Sulfur-Codoped TiO_2. *The Journal of Physical Chemistry C*, **112**, 6620-6626. http://dx.doi.org/10.1021/jp7110007

[35] Cao, Y.Q., Hu, Y.Y., Sun, J. and Hou, B. (2010) Explore Various Co-Substrates for Simultaneous Electricity Generation and Congo Red Degradation in Air-Cathode Single-Chamber Microbial Fuel Cell. *Bioelectrochemistry*, **79**, 71-76.

http://dx.doi.org/10.1016/j.bioelechem.2009.12.001

[36] Fu, S.S., Niu, H.L., Tao, Z.Y., Song, J.M., Mao, C.J., Zhang, S.Y., Chen, C.L. and Wang, D. (2013) Low Temperature Synthesis and Photocatalytic Property of Perovskite-Type $LaCoO_3$ Hollow Spheres. *Journal of Alloys and Compounds*, **576**, 5-12. http://dx.doi.org/10.1016/j.jallcom.2013.04.092